EUROPEAN ORGANISATION FOR NUCLEAR RESEARCH

CERN-PPE/92-34
28 February 1992

Evidence for b–flavoured Baryon Production in Z^0 Decays at LEP

The OPAL Collaboration

Abstract

We observe evidence for the production of b–flavoured baryons in decays of the Z^0 boson with the OPAL detector at LEP. We find 68 $\Lambda\ell^-$, $\overline{\Lambda}\ell^+$ candidates and 13 $\Lambda\ell^+$, $\overline{\Lambda}\ell^-$ candidates in 458 583 hadronic Z^0 decays. We interpret this as a signal of $55\pm9^{+0.3}_{-3.1}$ events from the semi-leptonic decays of b baryons. Assuming weakly decaying b baryons produced in Z^0 decays are mostly Λ_b particles, we measure the product branching ratio $\Gamma_{b\overline{b}}/\Gamma_{had} \cdot f(b \to \Lambda_b) \cdot B(\Lambda_b \to \Lambda\ell^-\overline{\nu}X)$, averaged over the electron and muon channels, to be $(6.2 \pm 1.0 \pm 1.5) \times 10^{-4}$.

(Submitted to Physics Letters B)

P.D. Acton[25], G. Alexander[23], J. Allison[16], P.P. Allport[5], K.J. Anderson[9], S. Arcelli[2], P. Ashton[16], A. Astbury[28], D. Axen[29], G. Azuelos[18,a], G.A. Bahan[16], J.T.M. Baines[16], A.H. Ball[17], J. Banks[16], G.J. Barker[13], R.J. Barlow[16], J.R. Batley[5], G. Beaudoin[18], A. Beck[23], J. Becker[10], T. Behnke[27], K.W. Bell[20], G. Bella[23], P. Berlich[10], S. Bethke[11], O. Biebel[3], U. Binder[10], I.J. Bloodworth[1], P. Bock[11], B. Boden[3], H.M. Bosch[11], S. Bougerolle[29], B.B. Brabson[12], H. Breuker[8], R.M. Brown[20], R. Brun[8], A. Buijs[8], H.J. Burckhart[8], P. Capiluppi[2], R.K. Carnegie[6], A.A. Carter[13], J.R. Carter[5], C.Y. Chang[17], D.G. Charlton[8], P.E.L. Clarke[25], I. Cohen[23], W.J. Collins[5], J.E. Conboy[15], M. Cooper[22], M. Couch[1], M. Coupland[14], M. Cuffiani[2], S. Dado[22], G.M. Dallavalle[2], S. De Jong[8], P. Debu[21], L.A. del Pozo[5], M.M. Deninno[2], A. Dieckmann[11], M. Dittmar[4], M.S. Dixit[7], E. do Conto el Silva[12], E. Duchovni[26], G. Duckeck[11], I.P. Duerdoth[16], D.J.P. Dumas[6], P.A. Elcombe[5], P.G. Estabrooks[6], E. Etzion[23], H.G. Evans[9], F. Fabbri[2], M. Fincke-Keeler[28], H.M. Fischer[3], D.G. Fong[17], C. Fukunaga[24,b], A. Gaidot[21], O. Ganel[26], J.W. Gary[4], J. Gascon[18], R.F. McGowan[16], N.I. Geddes[20], C. Geich-Gimbel[3], S.W. Gensler[9], F.X. Gentit[21], G. Giacomelli[2], V. Gibson[5], W.R. Gibson[13], J.D. Gillies[20], J. Goldberg[22], M.J. Goodrick[5], W. Gorn[4], C. Grandi[2], F.C. Grant[5], J. Hagemann[27], G.G. Hanson[12], M. Hansroul[8], C.K. Hargrove[7], P.F. Harrison[13], J. Hart[5], P.M. Hattersley[1], M. Hauschild[8], C.M. Hawkes[8], E. Heflin[4], R.J. Hemingway[6], R.D. Heuer[8], J.C. Hill[5], S.J. Hillier[1], D.A. Hinshaw[18], C. Ho[4], J.D. Hobbs[8], P.R. Hobson[25], D. Hochman[26], R.J. Homer[1], A.K. Honma[28,a], S.R. Hou[17], C.P. Howarth[15], R.E. Hughes-Jones[16], R. Humbert[10], P. Igo-Kemenes[11], H. Ihssen[11], D.C. Imrie[25], A.C. Janissen[6], A. Jawahery[17], P.W. Jeffreys[20], H. Jeremie[18], M. Jimack[2], M. Jobes[1], R.W.L. Jones[13], P. Jovanovic[1], D. Karlen[6], K. Kawagoe[24], T. Kawamoto[24], R.K. Keeler[28], R.G. Kellogg[17], B.W. Kennedy[15], D.E. Klem[19], T. Kobayashi[24], T.P. Kokott[3], S. Komamiya[24], L. Köpke[8], J.F. Kral[8], R. Kowalewski[6], H. Kreutzmann[3], J. von Krogh[11], J. Kroll[9], M. Kuwano[24], P. Kyberd[13], G.D. Lafferty[16], F. Lamarche[18], W.J. Larson[4], J.G. Layter[4], P. Le Du[21], P. Leblanc[18], A.M. Lee[17], M.H. Lehto[15], D. Lellouch[26], P. Lennert[11], C. Leroy[18], J. Letts[4], S. Levegrün[3], L. Levinson[26], S.L. Lloyd[13], F.K. Loebinger[16], J.M. Lorah[17], B. Lorazo[18], M.J. Losty[7], X.C. Lou[12], J. Ludwig[10], M. Mannelli[8], S. Marcellini[2], G. Maringer[3], A.J. Martin[13], J.P. Martin[18], T. Mashimo[24], P. Mättig[3], U. Maur[3], J. McKenna[28], T.J. McMahon[1], J.R. McNutt[25], F. Meijers[8], D. Menszner[11], F.S. Merritt[9], H. Mes[7], A. Michelini[8], R.P. Middleton[20], G. Mikenberg[26], J. Mildenberger[6], D.J. Miller[15], R. Mir[12], W. Mohr[10], C. Moisan[18], A. Montanari[2], T. Mori[24], M.W. Moss[16], T. Mouthuy[12,c], B. Nellen[3], H.H. Nguyen[9], S.W. O'Neale[8,d], B.P. O'Neill[4], F.G. Oakham[7], F. Odorici[2], M. Ogg[6], H.O. Ogren[12], H. Oh[4], C.J. Oram[28,a], M.J. Oreglia[9], S. Orito[24], J.P. Pansart[21], B. Panzer-Steindel[8], P. Paschievici[26], G.N. Patrick[20], S.J. Pawley[16], P. Pfister[10], J.E. Pilcher[9], D. Pitman[28], D.E. Plane[8], P. Poffenberger[28], B. Poli[2], A. Pouladdej[6], E. Prebys[8], T.W. Pritchard[13], H. Przysiezniak[18], G. Quast[27], M.W. Redmond[9], D.L. Rees[1], K. Riles[4], S.A. Robins[13], D. Robinson[8], A. Rollnik[3], J.M. Roney[9], E. Ros[8], S. Rossberg[10], A.M. Rossi[2,e], M. Rosvick[28], P. Routenburg[6], K. Runge[10], O. Runolfsson[8], D.R. Rust[12], S. Sanghera[6], M. Sasaki[24], A.D. Schaile[10], O. Schaile[10], W. Schappert[6], P. Scharff-Hansen[8], P. Schenk[28], H. von der Schmitt[11], S. Schreiber[3], J. Schwiening[3], W.G. Scott[20], M. Settles[12], B.C. Shen[4], P. Sherwood[15], R. Shypit[29], A. Simon[3], P. Singh[13], G.P. Siroli[2], A. Skuja[17], A.M. Smith[8], T.J. Smith[8], G.A. Snow[17], R. Sobie[28,f], R.W. Springer[17], M. Sproston[20], K. Stephens[16], R. Ströhmer[11], D. Strom[9,g], H. Takeda[24], T. Takeshita[24,h], P. Taras[18], S. Tarem[26], P. Teixeira-Dias[11], N.J. Thackray[1], G. Transtromer[25], T. Tsukamoto[24], M.F. Turner[5], G. Tysarczyk-Niemeyer[11], D. Van den plas[18], R. Van Kooten[8], G.J. VanDalen[4], G. Vasseur[21], C.J. Virtue[19], A. Wagner[27], D.L. Wagner[9], C. Wahl[10], J.P. Walker[1], C.P. Ward[5], D.R. Ward[5],

P.M. Watkins[1], A.T. Watson[1], N.K. Watson[8], M. Weber[11], P. Weber[6], S. Weisz[8], P.S. Wells[8], N. Wermes[11], M.A. Whalley[1], G.W. Wilson[21], J.A. Wilson[1], I. Wingerter[8], V-H. Winterer[10], T. Wlodek[26], N.C. Wood[16], S. Wotton[11], T.R. Wyatt[16], R. Yaari[26], Y. Yang[4,i], G. Yekutieli[26], M. Yurko[18], W. Zeuner[8], G.T. Zorn[17].

[1]School of Physics and Space Research, University of Birmingham, Birmingham, B15 2TT, UK
[2]Dipartimento di Fisica dell' Università di Bologna and INFN, Bologna, 40126, Italy
[3]Physikalisches Institut, Universität Bonn, D-5300 Bonn 1, FRG
[4]Department of Physics, University of California, Riverside, CA 92521 USA
[5]Cavendish Laboratory, Cambridge, CB3 0HE, UK
[6]Carleton University, Dept of Physics, Colonel By Drive, Ottawa, Ontario K1S 5B6, Canada
[7]Centre for Research in Particle Physics, Carleton University, Ottawa, Ontario K1S 5B6, Canada
[8]CERN, European Organisation for Particle Physics, 1211 Geneva 23, Switzerland
[9]Enrico Fermi Institute and Department of Physics, University of Chicago, Chicago Illinois 60637, USA
[10]Fakultät für Physik, Albert Ludwigs Universität, D-7800 Freiburg, FRG
[11]Physikalisches Institut, Universität Heidelberg, Heidelberg, FRG
[12]Indiana University, Dept of Physics, Swain Hall West 117, Bloomington, Indiana 47405, USA
[13]Queen Mary and Westfield College, University of London, London, E1 4NS, UK
[14]Birkbeck College, London, WC1E 7HV, UK
[15]University College London, London, WC1E 6BT, UK
[16]Department of Physics, Schuster Laboratory, The University, Manchester, M13 9PL, UK
[17]Department of Physics and Astronomy, University of Maryland, College Park, Maryland 20742, USA
[18]Laboratoire de Physique Nucléaire, Université de Montréal, Montréal, Quebec, H3C 3J7, Canada
[19]National Research Council of Canada, Herzberg Institute of Astrophysics, Ottawa, Ontario K1A 0R6, Canada
[20]Rutherford Appleton Laboratory, Chilton, Didcot, Oxfordshire, OX11 0QX, UK
[21]DPhPE, CEN Saclay, F-91191 Gif-sur-Yvette, France
[22]Department of Physics, Technion-Israel Institute of Technology, Haifa 32000, Israel
[23]Department of Physics and Astronomy, Tel Aviv University, Tel Aviv 69978, Israel
[24]International Centre for Elementary Particle Physics and Dept of Physics, University of Tokyo, Tokyo 113, and Kobe University, Kobe 657, Japan
[25]Brunel University, Uxbridge, Middlesex, UB8 3PH UK
[26]Nuclear Physics Department, Weizmann Institute of Science, Rehovot, 76100, Israel
[27]Universität Hamburg/DESY, II Inst für Experimental Physik, 2000 Hamburg 52, Germany
[28]University of Victoria, Dept of Physics, P O Box 3055, Victoria BC V8W 3P6, Canada
[29]University of British Columbia, Dept of Physics, 6224 Agriculture Road, Vancouver BC V6T 1Z1, Canada

[a]Also at TRIUMF, Vancouver, Canada V6T 2A3
[b]Now at Meiji Gakuin University, Yokohama 244, Japan

[c]Now at Centre de Physique des Particules de Marseille, Faculté des Sciences de Luminy, Marseille
[d]On leave from Birmingham University, Birmingham B15 2TT, UK
[e]Now at Dipartimento di Fisica, Università della Calabria and INFN, 87036 Rende, Italy
[f]And IPP, McGill University, High Energy Physics Department, 3600 University Str, Montreal, Quebec H3A 2T8, Canada
[g]Now at Dept of Physics, University of Oregon, Eugene, Oregon 97405
[h]Also at Shinshu University, Matsumoto 390, Japan
[i]On leave from Research Institute for Computer Peripherals, Hangzhou, China

1 Introduction

The quark model [1] has long predicted the existence of b-flavoured baryons, while evidence for b baryons has been reported only very recently [2, 3]. In this letter we present further evidence for b baryons, produced in hadronic decays of the Z^0 and observed in the OPAL detector at LEP.

Due to the large b quark mass, leptons resulting from semi-leptonic b hadron decays tend to have large momentum and high transverse momentum relative to the b hadron direction. Other leptons in Z^0 decays do not in general have this property. In analogy to $\Lambda_c^+ \to \Lambda X$ decays (X=anything), the Λ_b is expected to decay predominantly into the Λ_c^+. Considering the large branching fraction measured for $\Lambda_c^+ \to \Lambda X$ [4], a large fraction of Λ_b decays will produce a Λ; similar decay chains are expected for other b baryons. The Λ_c^+ and Λ retain large fractions of the momenta of the Λ_b and Λ_c^+ , respectively, so that the Λ particles are expected to be produced with large momenta. Fragmentation processes are expected to produce Λ particles of much lower momenta.

Semi-leptonic decays of b baryons are expected to produce $\Lambda\ell^-$ and $\overline{\Lambda}\ell^+$ pairs but not $\Lambda\ell^+$ and $\overline{\Lambda}\ell^-$ pairs, where ℓ is a charged lepton (electron or muon in this analysis). Thus a signature for b baryons is the correlation between the sign of the baryon number of a Λ particle and the sign of the electric charge of an associated lepton. Through the rest of this letter charge conjugation is implied. The strength of the method based on $\Lambda\ell^-$ correlation lies in the three-fold selection power of requiring energetic leptons, energetic Λ particles, and their correlation. Most other sources of leptons and Λ particles have no such correlation. By subtracting the wrong sign combinations from our signal, we are able to correct for these sources of background.

In this paper, we assume weakly decaying b baryons produced in Z^0 decays are mostly Λ_b particles. Given this assumption it is possible to calculate the product branching fraction $\Gamma_{b\overline{b}}/\Gamma_{had} \cdot f(b \to \Lambda_b) \cdot B(\Lambda_b \to \Lambda\ell^-\overline{\nu}X)$, where $\Gamma_{b\overline{b}}$ is the partial width for $Z^0 \to b\overline{b}$; Γ_{had} is the total hadronic width of the Z^0, and $f(b \to \Lambda_b)$ is the number of Λ_b hadrons produced per b quark in Z^0 decays.

2 The OPAL detector and hadronic event selection

The OPAL detector has been described in detail in an earlier publication [5]. Here we briefly describe detector components crucial to this analysis.

Tracking of charged particles is performed by the central detector, consisting of a jet chamber, a vertex detector, and chambers measuring the z coordinates[1] of tracks as they leave the jet chamber. The central detector is positioned inside a solenoidal coil, which provides a uniform magnetic field of 0.435 T. The jet chamber is a large volume drift chamber, 4 m in length and 3.7 m in diameter, divided into 24 azimuthal sectors with 159 layers of wires. The coil is

[1]The OPAL coordinate system is defined with positive z along the electron beam direction, θ and ϕ being the polar and azimuthal angles.

surrounded by a time-of-flight counter array and a lead glass electromagnetic calorimeter with a presampler. Outside the electromagnetic calorimeter is the instrumented return yoke of the magnet, forming the hadron calorimeter, and beyond this are muon chambers.

This analysis is based on about a half million hadronic decays of the Z^0 boson recorded with the OPAL detector during the 1990 and 1991 LEP runs. The data were collected in e^+e^- annihilation at centre-of-mass energies between 88.3 and 94.3 GeV. After data quality selection and detector performance requirements, we select 458 583 events. The OPAL criteria for the selection of hadronic Z^0 decay events have been described in detail elsewhere [6]. The track selection criteria used in this analysis are more stringent than those described in [6]. We require that events contain five or more tracks in order to reduce background from $e^+e^- \to \tau^+\tau^-$ events to a negligible level. The efficiency of the hadronic event selection criteria is determined to be 97%.

3 Identification of leptons and Λ particles

We first divide the event into jets. All good central detector tracks and energy clusters in the electromagnetic calorimeters which are not associated with tracks are used in the jet-finding procedure. We use the scaled-mass jet finding algorithm of JADE [7], with the E_0 recombination scheme [8] using a value of 0.04 for the jet resolution parameter $y_{\rm cut}$. In this analysis, the track of the lepton candidate is included in the calculation of the jet axis. The transverse momentum, $p_{\rm T}$, of each lepton candidate is calculated with respect to the axis of the jet to which it is associated.

The electron identification procedure used in this paper is the same as that described in a previous publication [9], and more details are given in a forthcoming paper [10]. The electron identification uses ionization energy loss, $\mathrm{d}E/\mathrm{d}x$, measured in the jet chamber [11], shower shape information from the electromagnetic calorimeter and presampler, and E/p, where E is the energy deposited in the calorimeter around the extrapolated track, which has a measured momentum p. The identification efficiency varies between 50% and 55% within $|\cos\theta| < 0.7$ in the kinematic range relevant to this analysis. The probability to misidentify a hadron as an electron is of the order of 0.1%. Electron candidates from photon conversions with an e^+e^- invariant mass of less than 50 MeV/c^2 are rejected in this analysis.

Muons are identified by associating central detector tracks to track segments in the muon detector. The position of a central detector track extrapolated to the muon detector is required to match a muon detector track segment in two dimensions. In addition, loose requirements on $\mathrm{d}E/\mathrm{d}x$ were made to reject kaons and protons. This combination of cuts gives an average identification efficiency of approximately 70% for muons with $p > 3$ GeV/c in the range $|\cos\theta| < 0.9$. Hadrons may fake prompt muons either by being misidentified or by pions and kaons decaying in flight to muons. The average probability for a hadron to fake a prompt muon in this kinematic range is estimated to be 0.8%.

The Λ particle is reconstructed via its $\Lambda \to p\pi^-$ decay. Two oppositely signed tracks are fitted to a common vertex. To improve invariant mass resolution, we demand that each track has a well measured z coordinate at the exit of the central detector. The distance between

the vertex position and the beam axis is required to be larger than 5 cm in order to reduce combinatorial background. The larger momentum track is taken to be the proton, and it is required to have dE/dx measurement compatible with that expected for a proton to reject background from $K^0_s \to \pi^+\pi^-$ decays. The other track is taken to be a pion and is required to have a distance of closest approach to the beam axis larger than 1 mm, to be consistent with being a secondary track. Finally, the momentum vector of the Λ candidate should extrapolate back approximately to the primary vertex. We demand that $|\theta_\Lambda| < 14$ mrad, where θ_Λ is the angle between the Λ momentum vector and the line connecting the primary vertex position to the Λ decay vertex in the plane perpendicular to the beam axis. This requirement rejects 25% of fake Λ vertices with an efficiency of 98% for real Λ particles with momentum greater than 4 GeV/c, according to a Monte Carlo simulation. The average efficiency for reconstructing $\Lambda \to p\pi^-$ with momentum greater than 4 GeV/c is estimated to be 29% by our Monte Carlo simulation.

In Figure 1, the $p\pi^-$ invariant mass distribution for Λ candidates with $p_\Lambda > 4$ GeV/c is shown. The mass and width obtained from fitting the distribution, using a Gaussian for the signal region above a fifth order polynomial background distribution, are 1115.8±0.4 MeV/c^2 and 2.6±0.2 MeV/c^2, respectively. The fitted mass agrees well with the world average of 1115.63 MeV/c^2 [12]. A total of 7033 ± 292 $\Lambda \to p\pi^-$ decays are estimated by the fit in Figure 1.

4 Study of Λ-lepton correlations

We search for Λ candidates inside a cone of half-angle 50° about each lepton candidate. A Monte Carlo simulation indicates that this angular cut is 99% efficient for $\Lambda_b \to \Lambda\ell^-\overline{\nu}X$ decays and rejects 99% of Λ-lepton combinations where the Λ and lepton have resulted from the decays of different b hadrons in the same event.

There are several possible sources of background producing $\Lambda\ell$ candidates that do not result from the decay of b baryons:

1. The decays of B mesons to Λ_c^+, $\overline{B} \to \Lambda_c^+\overline{N}\ell^-\overline{\nu}X$, where $\overline{N}$ is an anti-baryon.
2. The semi-leptonic decay $\Lambda_c^+ \to \Lambda\ell^+\nu X$.
3. Associated production of Λ particles and anti-baryons, where an anti-proton resulting from the anti-baryon is misidentified as an e^- or a μ^-.
4. Random association of Λ particles produced in the fragmentation process with leptons from decays of c hadrons and b hadrons.
5. Genuine Λ particles randomly paired with fake leptons
6. Genuine leptons randomly combined with fake Λ particles.

Using a Monte Carlo simulation, we estimate the reconstruction efficiency for $\Lambda_b \to \Lambda\ell^-\overline{\nu}X$ and study some of these backgrounds. The JETSET 7.2 parton shower Monte Carlo generator [13] is used to simulate the decay $Z^0 \to b\overline{b}$. The fragmentation is performed using the symmetric LUND fragmentation function with parameters tuned to describe the inclusive distributions of

hadronic Z^0 decays [14]. The mean fractional energy of the primary b hadrons, $\langle x_E \rangle$, is 0.74 in this simulation, where $x_E = E_B/E_{beam}$ and E_B is the energy of the primary b hadron. The Λ_b mass is assumed to be 5.62 GeV/c^2, consistent with theoretical calculations [15]. Events containing semi-leptonic decays of the Λ_b or the Λ_c^+ producing Λe or $\Lambda\mu$, where $\Lambda \rightarrow p\pi^-$, are subjected to a full simulation of the detector response and event reconstruction [16]. For background studies we use the EURODEC program [17] to simulate the decay $\overline{B} \rightarrow \Lambda_c^+ \overline{N} \ell^- \overline{\nu} X$, where the B mesons are generated with the JETSET 7.2 program.

The $\Lambda\ell$ selection criteria are chosen to reduce contamination from each of these processes. In Figure 2 we show the predicted momentum spectrum of Λ particles produced by fragmentation in $Z^0 \rightarrow b\overline{b}$ events and that of Λ particles resulting from b baryon decays. The b baryon decays produce a hard Λ momentum spectrum. The Monte Carlo simulation shows that 83% of fragmentation Λ particles produced in $Z^0 \rightarrow b\overline{b}$ events are rejected by the cut

- $p_\Lambda > 4$ GeV/c

while accepting 84% of Λ particles from the decay of b baryons. The p_T distributions for leptons from the decays $\Lambda_b \rightarrow \Lambda_c^+ \ell^- \overline{\nu} X$, $\overline{B} \rightarrow \Lambda_c^+ \overline{N} \ell^- \overline{\nu} X$ and $\Lambda_c^+ \rightarrow \Lambda \ell^+ \nu X$ are shown in Figure 3. The leptons are required to satisfy the requirements

- $p > 3$ GeV/c and $p_T > 0.8$ GeV/c

in order to enhance the contribution from the semi-leptonic decays of b hadrons relative to the other sources. About 60% of the semi-leptonic b baryon decays are expected to pass the p and p_T cuts. Shown in Figure 4 are the expected distributions of $m_{\Lambda\ell}$, the invariant mass of the $\Lambda\ell$ pairs, for the three processes listed above after the p_Λ, p and p_T cuts. The criterion

- $m_{\Lambda\ell} > 2.2$ GeV/c^2

highly suppresses the remaining background contributions and has an expected efficiency of 83%. Furthermore the requirement

- $p_{\Lambda\ell} > 9$ GeV/c

where $p_{\Lambda\ell}$ is the momentum of the $\Lambda\ell$ pairs, rejects 15% of the remaining combinatorial background caused by Λ particles produced in the fragmentation process combined with fake leptons or leptons resulting from processes other than b hadron decays. The efficiency for this momentum cut is determined to be 99% by our Monte Carlo simulation.

In baryonic B meson decays, an anti-baryon must accompany the Λ_c^+ baryon in order to conserve baryon number. Consequently, the distributions of lepton p_T and $\Lambda\ell^-$ invariant mass should be much softer than those for $\Lambda\ell^-$ pairs from b baryon decays. The $p_T > 0.8$ GeV/c and $m_{\Lambda\ell} > 2.2$ GeV/c^2 requirements should reject 96% of this background. The ARGUS experiment has reported an upper limit of 1.6×10^{-3} at 90% confidence level (C L) for $B(\overline{B} \rightarrow p\ell^-\overline{\nu}X)$ [18].

The CLEO experiment has investigated the inclusive baryonic decays of the B meson and concluded that half of the protons produced in B meson decays were from the decay of Λ particles [4]. If we assume that half of the decays $\overline{B} \rightarrow p\ell^-\overline{\nu}X$ proceed via $\overline{B} \rightarrow \Lambda\ell^-\overline{\nu}X$, then the ARGUS limit on $B(\overline{B} \rightarrow p\ell^-\overline{\nu}X)$ translates to a 90% C L upper limit of 1.2×10^{-3} for $B(\overline{B} \rightarrow \Lambda\ell^-\overline{\nu}X)$. Using the Standard Model value of 0.217 for $\Gamma_{b\overline{b}}/\Gamma_{had}$ [19] and assuming that all b quarks form a B meson, this translates into 1.6 ± 0.5 $\Lambda\ell^-$ events from semi-leptonic baryonic B meson decays in our data sample of Z^0 decays, where the error comes from Monte Carlo statistics.

Semi-leptonic decays of the Λ_c^+ contribute only to the $\Lambda\ell^+$ type events. The criteria $p_T > 0.8$ GeV/c and $m_{\Lambda\ell} > 2.2$ GeV/c^2 are expected to reject 99.9% of this background. We assume that Λ_c^+ production rates are 10% per c quark in $Z^0 \rightarrow c\overline{c}$ events and 20% per b quark in $Z^0 \rightarrow b\overline{b}$ events to estimate this background quantitatively. Using the 90% C L limit of 2.4×10^{-2} for the branching ratio for $\Lambda_c^+ \rightarrow \Lambda e^+X$ [12], we estimate that the contribution from background (2) to the $\Lambda\ell^+$ events is of the order of 0.3 events.

An anti-baryon produced in association with a Λ, when misidentified as either an e^- or a μ^-, may produce a candidate for a $\Lambda\ell^-$ pair. This background is potentially serious since it gives the same $\Lambda\ell$ combination as the Λ_b signal. The events in the Λ signal region of Figure 1 are used for the estimate of this background. The proton tracks from these Λ candidates are subjected to the lepton identification procedure and the kinematic selection criteria for leptons. We find 3 proton tracks which are misidentified as electrons or muons. Assuming half of the final state anti-baryons are anti-protons, we expect 1.5 $\Lambda\ell^-$ events arising from Λ anti-baryon association. This estimate is conservative because the $p_{\Lambda\ell}$ and $m_{\Lambda\ell}$ cuts have not been taken into account.

For backgrounds (4), (5) and (6), we assume there is no correlation between the baryon number of the Λ and the lepton charge. Thus their contribution is accounted for by the wrong sign subtraction. This assumption will be examined in Section 6. Furthermore, these backgrounds are suppressed by the $\Lambda\ell$ selection criteria.

In summary, we expect less than 3.1 events contributing to only $\Lambda\ell^-$ events and 0.3 events contributing to only $\Lambda\ell^+$ events. The other sources of background contribute equally to $\Lambda\ell^-$ and $\Lambda\ell^+$ type events.

The $p\pi^-$ mass distributions for the $\Lambda\ell^-$ and $\Lambda\ell^+$ combinations, selected as above, are shown in Figures 5a and 5b, respectively. We define the signal band as the region centred at the nominal Λ mass of 1115.6 MeV/c^2 with a half width of 3σ, where σ is 2.6 MeV/c^2 as obtained from Figure 1. We observe 26 Λe^-, 5 Λe^+, 42 $\Lambda\mu^-$, and 8 $\Lambda\mu^+$ candidates. Subtracting the $\Lambda\ell^+$ from the $\Lambda\ell^-$ candidates, we observe excesses of 21.0 ± 5.6 Λe^- and 34.0 ± 7.1 $\Lambda\mu^-$ pairs.

In total we observe an excess of 55 $\Lambda\ell^-$ pairs over 13 $\Lambda\ell^+$ candidates. The probability for a statistical fluctuation to produce the observed excess is negligible, even allowing for the estimated extra background of 3.1 events for the $\Lambda\ell^-$. The distributions of the $\Lambda\ell$ mass and the lepton p_T for the $\Lambda\ell^-$ pairs, after $\Lambda\ell^+$ subtraction, agree well with Monte Carlo predictions as shown in Figures 6a and 6b. As the background contributions specific to $\Lambda\ell^-$ and $\Lambda\ell^+$ are upper limits we do not subtract these backgrounds from the excess $\Lambda\ell^-$ events, but include them as a systematic error. The number of $\Lambda\ell^-$ events resulting from semi-leptonic decays of b baryons is thus determined to be $55.0\pm9.0^{+0.3}_{-3.1}$. We conclude that this is strong evidence for

the semi-leptonic decays of b baryons into states containing a Λ particle.

5 Calculation of product branching ratio

Using the excess $\Lambda\ell^-$ events observed in the data, we measure the product branching ratio $\Gamma_{b\bar{b}}/\Gamma_{had} \cdot f(b \to \Lambda_b) \cdot B(\Lambda_b \to \Lambda\ell^-\overline{\nu}X)$ and estimate the production rate of b baryons in hadronic Z^0 decays.

The $\Lambda\ell^-$ detection efficiency is obtained from the fraction of generated $\Lambda_b \to \Lambda\ell^-\overline{\nu}X$ events that are reconstructed. In Figures 6c and 6d are shown the Λ and the lepton momentum distributions, respectively, for the $\Lambda\ell^-$ signal events and Monte Carlo predictions. These distributions are in adequate agreement above our kinematic cuts. The efficiencies do not exhibit a strong dependence on the Λ momentum. The overall efficiency is estimated to be $(4.0 \pm 0.2)\%$ for Λe^- and $(5.3 \pm 0.3)\%$ for $\Lambda\mu^-$, where the $\Lambda \to p\pi^-$ branching ratio is included [12] and the errors are statistical only.

Correcting for the selection efficiency, we obtain 525±138 Λe^- events and 642±134 $\Lambda\mu^-$ events. Normalizing these numbers to 458 583 hadronic Z^0 decays and correcting for the hadronic event selection efficiency, we extract

$$\Gamma_{b\bar{b}}/\Gamma_{had} \cdot f(b \to \Lambda_b) \cdot B(\Lambda_b \to \Lambda e^-\overline{\nu}_e X) = (5.6 \pm 1.5) \times 10^{-4} \text{ and}$$
$$\Gamma_{b\bar{b}}/\Gamma_{had} \cdot f(b \to \Lambda_b) \cdot B(\Lambda_b \to \Lambda\mu^-\overline{\nu}_\mu X) = (6.8 \pm 1.4) \times 10^{-4} \ .$$

Averaging over the two channels we measure

$$\Gamma_{b\bar{b}}/\Gamma_{had} \cdot f(b \to \Lambda_b) \cdot B(\Lambda_b \to \Lambda\ell^-\overline{\nu}X) = (6.2 \pm 1.0) \times 10^{-4} \ ,$$

where the error is statistical only.

To estimate the b baryon production rate, we assume weakly decaying b baryons produced in Z^0 decays are mostly Λ_b particles. Though the production of Ξ_b and Ω_b baryons is kinematically possible, their rates are expected to be suppressed by an order of magnitude since these baryons require creation of one or two $s\bar{s}$ pairs from the sea. This suppression can be seen for light baryons at lower energy e^+e^- collision experiments [20]. The Σ_b is expected to decay primarily to the Λ_b baryon radiatively or strongly if the mass difference between the two types of baryons is sufficiently large. The charged Σ_b baryon will decay weakly into Σ_c baryons if this mass difference is smaller than the pion mass, whereas Σ_c baryons couple exclusively to Λ_c^+ via radiative or strong decays [12, 21]. Therefore, stable c-flavoured baryons produced in semi-leptonic decays of the Λ_b baryon should be dominated by the charmed baryon Λ_c^+. The inclusive branching ratio $B(\Lambda_c^+ \to \Lambda X)$ is measured to be (45±15)% [4]. The semi-leptonic branching ratio of b baryons is expected to be similar to that of B mesons [22]. We assume (8.8±2.2)% for the branching ratio $B(\Lambda_b \to \Lambda_c^+\ell^-\overline{\nu}X)$. This is motivated by the following considerations: firstly, the average semi-leptonic branching ratio of B hadrons at LEP and at lower energies [23, 12, 24] is compatible with being 11% and; secondly, non-strange charmed mesons account

for about 80% [12] of the b $\rightarrow$ cX transitions in B meson decays. Thus in analogy to B meson decays, we assume a branching ratio of (80$\pm$20)% for the inclusive decay $\Lambda_b \rightarrow \Lambda_c^+ X$. This assumption allows for possible decays of the type $\Lambda_b \rightarrow Dp\ell^-\overline{\nu}X$. Based on these arguments and assumptions, we can calculate

$$f(b \rightarrow \Lambda_b) = \frac{N_{\Lambda\ell^-}}{2 \cdot (\Gamma_{b\bar{b}}/\Gamma_{had}) \cdot N_Z \cdot B(\Lambda_b \rightarrow \Lambda_c^+ \ell^- \overline{\nu} X) \cdot B(\Lambda_c^+ \rightarrow \Lambda X)} ,$$

where $N_{\Lambda\ell^-}$ is the efficiency corrected number of $\Lambda\ell^-$ events resulting from b baryon decays. Using a value of 0.217 for $\Gamma_{b\bar{b}}/\Gamma_{had}$ [19] and averaging over the e and μ channels, we find $f(b \rightarrow \Lambda_b)$=0.072$\pm$0.012, where the error is purely statistical.

6 Systematic errors

Given in Table 1 are the systematic uncertainties considered on the product branching ratio $\Gamma_{b\bar{b}}/\Gamma_{had} \cdot f(b \rightarrow \Lambda_b) \cdot B(\Lambda_b \rightarrow \Lambda\ell^-\overline{\nu}X)$.

Table 1. Systematic errors for product branching ratio

Sources of Systematics	Systematic Errors (%)
Uncertainties on fragmentation model	$\pm$10
Monte Carlo statistics	$\pm$5.5
Lepton identification	$\pm$10
Λ-finding efficiency	$\pm$14
Background estimates	$^{+0.5}_{-5.6}$
Correlations of fragmentation Λ particles	$\pm$9.6
Λ_b polarization	$\pm$6
Λ_b mass	$\pm$1.2
Modelling of semi-leptonic Λ_b decays	$\pm$2
Total	$\pm$24

We study the uncertainty in the fragmentation model by comparing the Peterson fragmentation with the LUND scheme of the Monte Carlo program JETSET 7.2. We adjust the fragmentation parameter of the Peterson fragmentation function to effectively vary $\langle x_E \rangle$ from 0.70 to 0.74. The largest difference in kinematic acceptance between the Peterson fragmentation and the LUND scheme (with $\langle x_E \rangle$=0.74) is 10%, which we take as the systematic error on the efficiency due to fragmentation. The statistical error on the $\Lambda\ell^-$ reconstruction efficiency from the full Monte Carlo simulation is 5.5% averaged over the electron and muon channels. We estimate an overall uncertainty of 10% in $\Lambda_b \rightarrow \Lambda\ell^-X$ reconstruction efficiency due to the identification of electrons and muons[2]. The uncertainty on the Λ-finding efficiency is conservatively estimated to be $\pm$14% by comparing the Monte Carlo distributions of variables used in

[2]The lepton identification is under study. The systematic uncertainty quoted in this letter is a very conservative estimate.

Λ reconstruction with those of the data. The systematic error due to background contributions to $\Lambda\ell^{\pm}$ was calculated in Section 4 and is $^{+0.5\%}_{-5.6\%}$. There may be some $\Lambda\ell^-$ correlation arising from background (4) (fragmentation Λ particles combined with real leptons from b decays). However, a fit to the wrong sign events yields a Λ signal of only 3.0±4.8 events. Using the JETSET 7.2 event generator, we find the ratio between $\Lambda\ell^-$ and $\Lambda\ell^+$ to be 1.68±0.15 assuming $f(b \to \Lambda_b)$=0. This ratio is found to be 0.97±0.09 with $f(b \to \Lambda_b)$ set at 7.6% per b quark. Assuming this ratio is 1.00±0.68, we find a systematic uncertainty of ±9.6% on the product branching ratio.

Polarization of the Λ_b should vary the lepton momentum spectrum and thus change the kinematic acceptance of leptons resulting from Λ_b decays. Based on the calculation of lepton spectra for different degrees of polarization [25], we estimate that this uncertainty is of the order of 6%. The mass of the Λ_b, calculated to lie in the range 5.60–5.63 GeV/c^2 [15], affects both the lepton p_T and $\Lambda\ell^-$ invariant mass. By varying the Λ_b mass by ± 40 MeV/c^2, a 1.2% variation in the $\Lambda\ell^-$ efficiency is found. We also examine the difference in acceptance between $\Lambda_b \to \Lambda_c^+\ell^-\overline{\nu}$ and $\Lambda_b \to \Lambda_c^+\ell^-\overline{\nu}\pi^+\pi^-$ to estimate the effect of semi-leptonic decays of Λ_b that contain other hadrons in addition to the Λ_c^+; such decays are not present in the standard JETSET 7.2. We find a 10% change in acceptance for our kinematic selection. Theoretical calculations indicate that $\Lambda_b \to \Lambda_c^+\ell^-\overline{\nu}$ is the highly favoured semi-leptonic decay mode; however, we cannot exclude other modes at the 20% level [22]. Thus we assign a 2% systematic error for the effect of additional particles in the semi-leptonic decays of Λ_b which are not present in our Monte Carlo simulation.

We combine these errors in quadrature to find an overall systematic error of ±24%. Thus we measure the product branching ratio $\Gamma_{b\overline{b}}/\Gamma_{had} \cdot f(b \to \Lambda_b) \cdot B(\Lambda_b \to \Lambda\ell^-\overline{\nu}X)$ to be $(6.2 \pm 1.0 \pm 1.5) \times 10^{-4}$.

Table 2. Systematic errors for Λ_b production rate

Sources of Systematics	Systematic Errors (%)
Uncertainties on product branching ratio	±24
$B(B \to \Lambda X)$	±33
$B(\Lambda_b \to \Lambda_c^+\ell^-\overline{\nu}X)$	±25
Total	±48

Listed in Table 2 are systematic errors on the estimated b baryon production rate per b quark. We combine in quadrature the systematic error of the product branching ratio with uncertainties in $B(B \to \Lambda X)$ and $B(\Lambda_b \to \Lambda_c^+\ell^-\overline{\nu}X)$ and find the overall systematic error to be ±48%. This results in a b baryon production rate per b quark of $f(b \to \Lambda_b) = 0.072 \pm 0.012 \pm 0.034$ in Z^0 decays, where the errors are statistical and systematic, respectively.

7 Conclusions

In conclusion, we observe 68 $\Lambda\ell^-$ candidates and 13 $\Lambda\ell^+$ candidates, which we interpret as a signal of $55.0\pm9.0^{+0.3}_{-3.1}$ $\Lambda\ell^-$ events from the semi-leptonic decay of b baryons into states

containing a Λ particle. This observation is strong evidence for the production of the b-flavoured baryon in hadronic decays of the Z^0 boson. Assuming weakly decaying b-flavoured baryons produced in the decays of the Z^0 are mostly Λ_b baryons, we measure the product branching ratio $\Gamma_{b\bar{b}}/\Gamma_{had} \cdot f(b \to \Lambda_b) \cdot B(\Lambda_b \to \Lambda \ell^- \overline{\nu} X)$, averaged over the electron and muon channels, to be $(6.2 \pm 1.0 \pm 1.5) \times 10^{-4}$, where the errors are statistical and systematic, respectively. We also estimate the b baryon production rate in Z^0 decays to be $0.072 \pm 0.012 \pm 0.034$ per b quark.

8 Acknowledgements

It is a pleasure to thank the SL Division for the efficient operation of the LEP accelerator and their continuing close cooperation with our experimental group. In addition to the support staff at our own institutions we are pleased to acknowledge the Department of Energy, USA, National Science Foundation, USA, Science and Engineering Research Council, UK, Natural Sciences and Engineering Research Council,Canada, Israeli Ministry of Science, Minerva Gesellschaft, Japanese Ministry of Education, Science and Culture (the Monbusho) and a grant under the Monbusho International Science Research Program, American Israeli Bi-national Science Foundation, Direction des Sciences de la Matière du Commissariat à l'Energie Atomique, France, Bundesministerium für Forschung und Technologie, FRG, A.P. Sloan Foundation and Junta Nacional de Investigação Científica e Tecnológica, Portugal.

References

[1] See, for example, S. Capstick and N. Isgur Phys. Rev. **D 34** (1986) 2809;
N. Isgur and M. B. Wise, Phys. Rev. Lett. **66** (1991) 1130.

[2] UA1 Collaboration, C. Albajar *et al.*, Phys. Lett. **B 273** (1991) 540.
Earlier claims have been disputed. See reference 12.

[3] ALEPH Collaboration, D. Decamp *et al.*, CERN-PPE/91-229, submitted to Phys. Lett.
Note that, in this reference, the symbol ℓ denotes the sum over electron and muon channels, instead of the average of these two channels as used in this letter.

[4] CLEO Collaboration, G. Crawford *et al.*, Phys. Rev. **D 45** (1992) 752.

[5] OPAL Collaboration, K. Ahmet *et al.*, Nucl. Instrum. and Meth. **A 305** (1991) 275.

[6] OPAL Collaboration, G. Alexander *et al.*, Z. Phys. **C 52** (1991) 175.

[7] JADE Collaboration, W. Bartel *et al.*, Z. Phys. **C 33** (1986) 23;
JADE Collaboration, S. Bethke *et al.*, Phys. Lett. **B 213** (1988) 235.

[8] OPAL Collaboration, M. Z. Akrawy *et al.*, Z. Phys. **C 49** (1991) 375.

[9] OPAL Collaboration, P. D. Acton *et al.*, CERN PPE/91-212, submitted to Phys. Lett.

[10] OPAL Collaboration, *A Measurement of Electron Production in Hadronic* Z^0 *Decays and a Determination of* $\Gamma(Z^0 \rightarrow b\bar{b})$, to be submitted to Z. Phys.

[11] M. Hauschild *et al.*, CERN-PPE/91-130, submitted to Nucl. Instrum. and Meth.

[12] Particle Data Group, J. J. Hernandez *et al.*, Phys. Lett. **B 239** (1990) 1.

[13] T. Sjöstrand, Comput. Phys. Commun. **39** (1986) 347;
T. Sjöstrand and M. Bengtsson, Comput. Phys. Commun. **43** (1987) 367;
T. Sjöstrand, Int. J. of Mod. Phys. **A 3** (1988) 751.

[14] OPAL Collaboration, M. Akrawy *et al.*, Z. Phys. **C 47** (1990) 505.

[15] W. Kwong and J. L. Rosner, Phys. Rev. **D 44** (1991) 212.

[16] J. Allison *et al.*, CERN-PPE/91-234, submitted to Nucl. Instrum. and Meth.

[17] M. Bosman *et al.*, MPI-PAE/PTh 49/89, August 1989.

[18] ARGUS Collaboration, H. Albrecht *et al.*, Phys. Lett. **B 249** (1990) 359.

[19] Standard Model prediction based on the line shape program ZFITTER, Dubna–Zeuthen radiative correction group,
D. Yu. Bardin *et al.*, Berlin–Zeuthen preprint PHE 89-19, 1989;
R. Kleiss *et al.*, *Z Physics at LEP1* , CERN 89-08, ed. G. Altarelli *et al.*, Vol. 3 (1989) 60.
In the fit, the masses used for the Z^0, the top quark and Higgs boson were M_Z=91.17 GeV/c^2, M_t=130 GeV/c^2 and M_{Higgs}=100 GeV/c^2.

[20] D. H. Saxon, Rutherford Appleton Laboratory preprint RAL-86-057, July 1986;
TASSO Collaboration, W. Braunschweig *et al.*, Z. Phys. **C 42** (1989) 189.

[21] CLEO Collaboration, T. Bowcock *et al.*, Phys. Rev. Lett. **62** (1989) 1240;
ARGUS Collaboration, H. Albrecht *et al.*, Phys. Lett. **B 211** (1988) 489.

[22] S. Rudaz and M. B. Voloshin, Phys. Lett. **B 252** (1990) 443;
N. Isgur and M. Wise, Nucl. Phys. **B 348** (1991) 276.

[23] ALEPH Collaboration, D. Decamp *et al.*, Phys. Lett. **B 244** (1990) 551;
DELPHI Collaboration, P. Abreu *et al.*, CERN-PPE/90-118, paper presented at the Singapore conference, August, 1990;
L3 Collaboration, B Adeva *et al.*, Phys. Lett. **B 261** (1991) 177;
OPAL Collaboration, M. Z. Akrawy *et al.*, Phys. Lett. **B 263** (1991) 311.

[24] CLEO Collaboration, S. Henderson *et al.*, Cornell Report CLNS 91/110.

[25] T. Mannel and G. A. Schuler, DESY 91-095, Sept 6, 1991.

Figure Captions

Figure 1: The $p\pi^-$ mass distribution for reconstructed secondary vertices satisfying the Λ selection criteria (see text) with $p_\Lambda > 4.0$ GeV/c.

Figure 2: The simulated momentum distribution of Λ particles from $Z^0 \to b\bar{b} \to \Lambda_b X$, $\Lambda_b \to \Lambda \ell^- X$ compared with that for Λ particles from the fragmentation process in $Z^0 \to b\bar{b}$ events. These distributions are normalised to the same area since the relative rate is unknown.

Figure 3: The lepton p_T distributions predicted by JETSET 7.2 for $\Lambda_b \to \Lambda_c^+ \ell^- \bar{\nu} X$, EURODEC for $\bar{B} \to \Lambda_c^+ \bar{N} \ell^- \bar{\nu} X$, and JETSET 7.2 for $\Lambda_c^+ \to \Lambda \ell^+ \nu X$. These distributions are normalised to the same area since the branching ratios for the latter two processes are unknown.

Figure 4: The Monte Carlo Λ-lepton invariant mass distribution for Λ-lepton pairs from:
$Z^0 \to b\bar{b} \to \Lambda_b X$, $\Lambda_b \to \Lambda \ell^- X$,
$Z^0 \to b\bar{b} \to \bar{B} X$, $\bar{B} \to \Lambda_c^+ \bar{N} \ell^- \bar{\nu} X$ and
$Z^0 \to c\bar{c} \to \Lambda_c^+ X$, $\Lambda_c^+ \to \Lambda \ell^+ \nu X$.
The criteria $p_\Lambda > 4$ GeV/c, and $p > 3$ GeV/c and $p_T > 0.8$ GeV/c for leptons are applied for these mass distributions. The change in the relative normalisation between Figure 3 and Figure 4 reflects the effect of these requirements.

Figure 5: **a.** The $p\pi^-$ invariant mass distribution of the Λ particles for Λe^- candidates (hatched histogram) and for $\Lambda \mu^-$ candidates (open histogram).
b. The $p\pi^-$ invariant mass distribution of the Λ particles for Λe^+ candidates (hatched histogram) and for $\Lambda \mu^+$ candidates (open histogram).

Figure 6: Distributions for the excess $\Lambda \ell^-$ pairs after subtraction of the $\Lambda \ell^+$ candidates. The data are shown together with predictions from Monte Carlo Λ_b events, generated with m_{Λ_b}=5.62 GeV/c^2.
a. The $\Lambda \ell^-$ invariant mass.
b. The lepton p_T with respect to the jet axis.
c. The Λ momentum.
d. The lepton momentum.

Figure 1

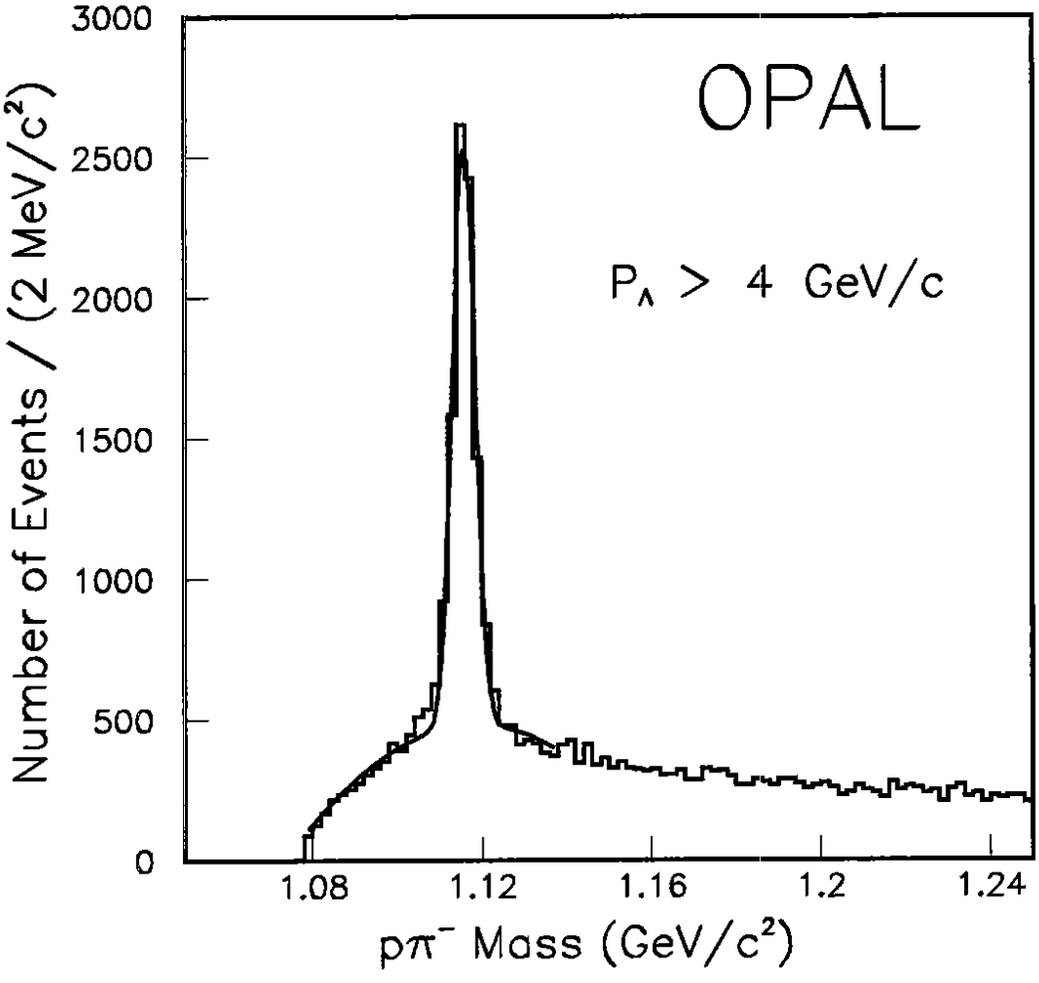
OPAL
$P_\Lambda > 4$ GeV/c
Number of Events / (2 MeV/c^2)
3000
2500
2000
1500
1000
500
0
1.08
1.12
1.16
1.2
1.24
$p\pi^-$ Mass (GeV/c^2)

Figure 2

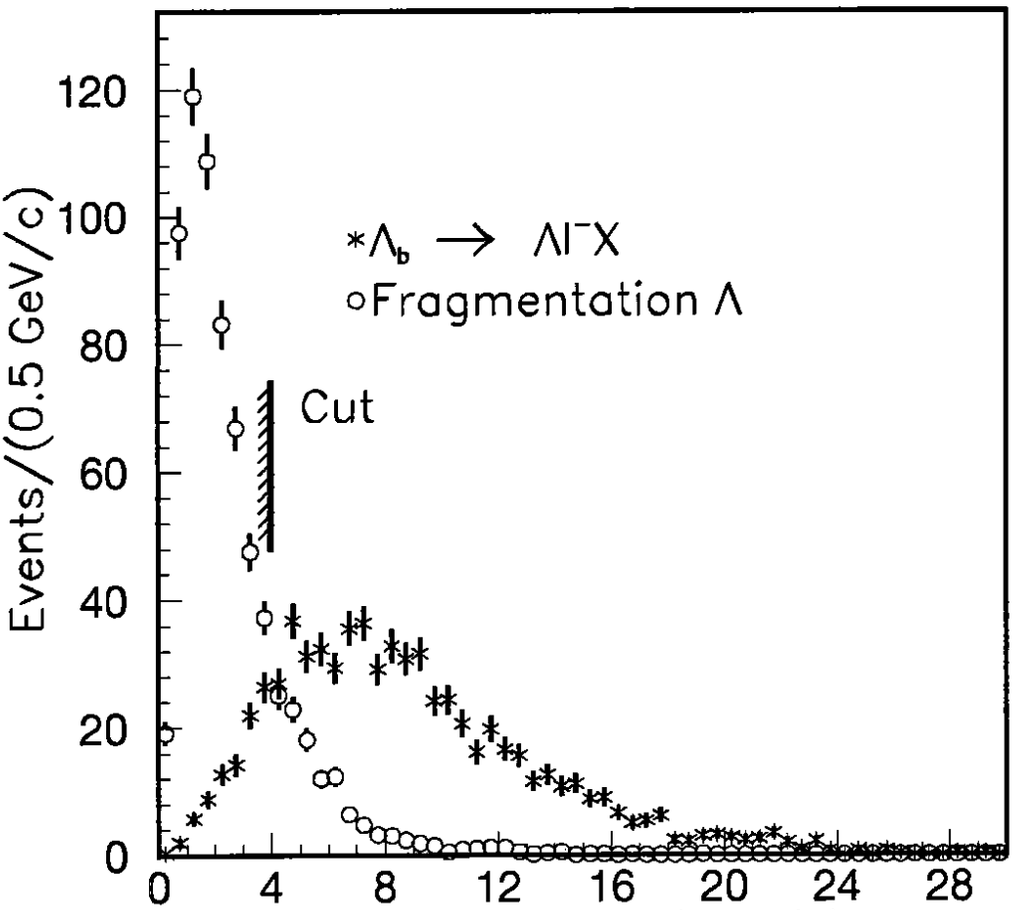
120
100
80
60
40
20
0
Events/(0.5 GeV/c)
*$\Lambda_b \rightarrow \Lambda l^- X$
oFragmentation Λ
Cut
0
4
8
12
16
20
24
28
Λ Momentum (GeV/c)

Figure 3

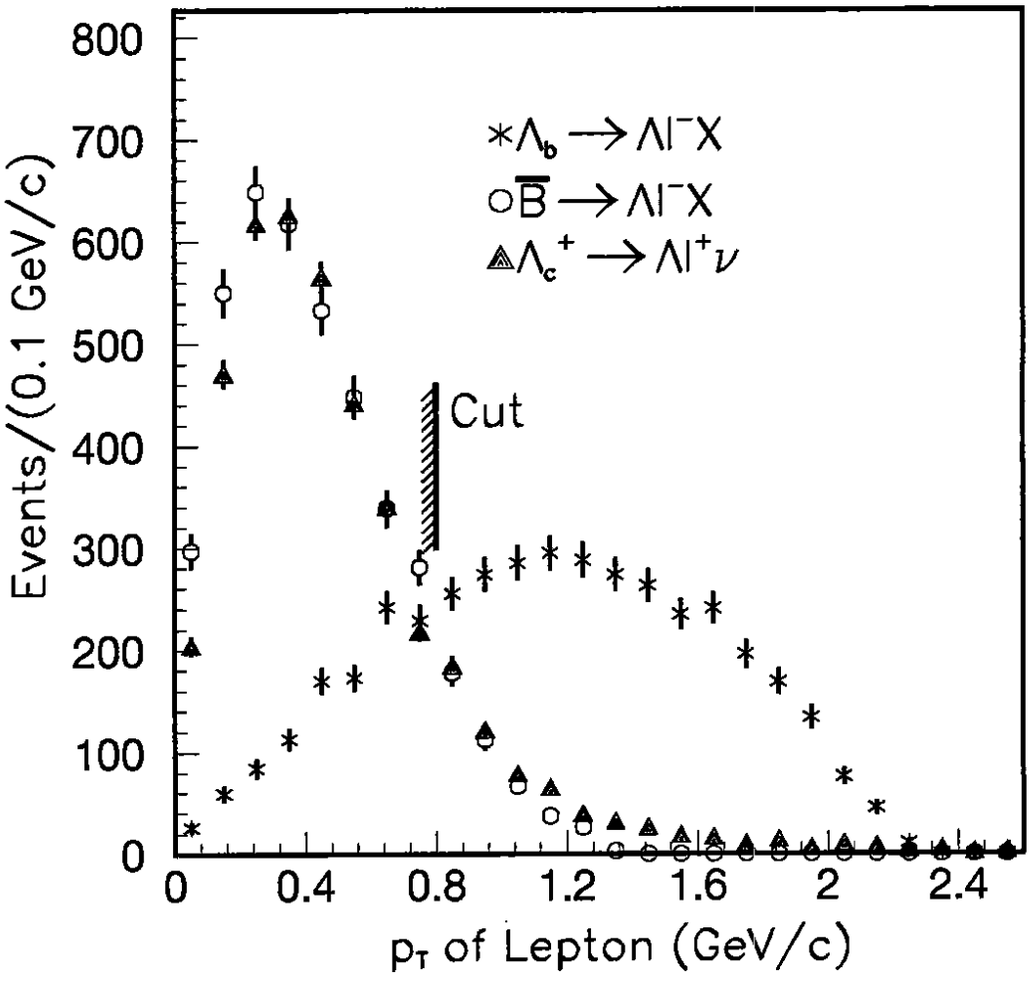
800
700
600
500
400
300
200
100
0
Events/(0.1 GeV/c)
0
0.4
0.8
1.2
1.6
2
2.4
p_T of Lepton (GeV/c)
$*\Lambda_b \rightarrow \Lambda l^- X$
$\circ \overline{B} \rightarrow \Lambda l^- X$
$\blacktriangle \Lambda_c^+ \rightarrow \Lambda l^+ \nu$
Cut

Figure 4

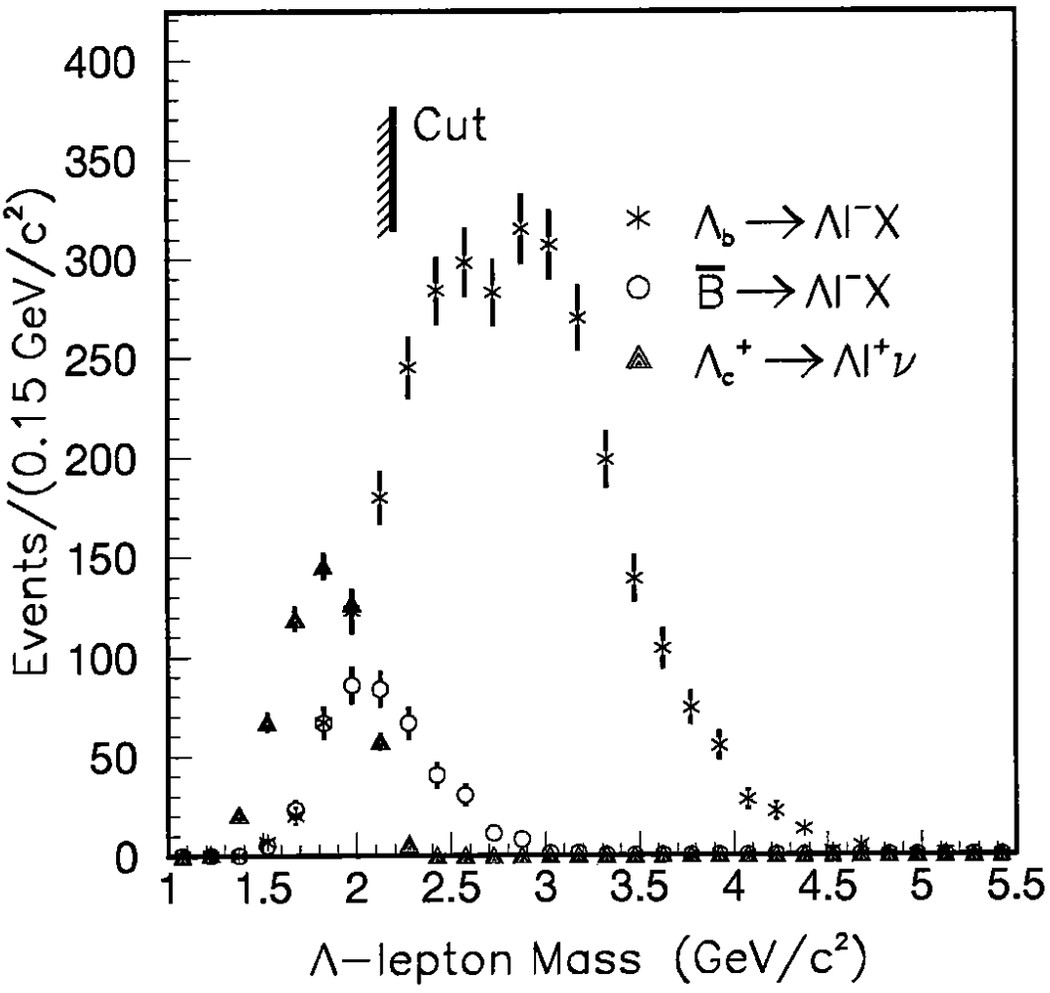
Cut
$\Lambda_b \rightarrow \Lambda l^- X$
$\bar{B} \rightarrow \Lambda l^- X$
$\Lambda_c^+ \rightarrow \Lambda l^+ \nu$
Events/(0.15 GeV/c^2)
0
50
100
150
200
250
300
350
400
1
1.5
2
2.5
3
3.5
4
4.5
5
5.5
Λ–lepton Mass (GeV/c^2)

Figure 5

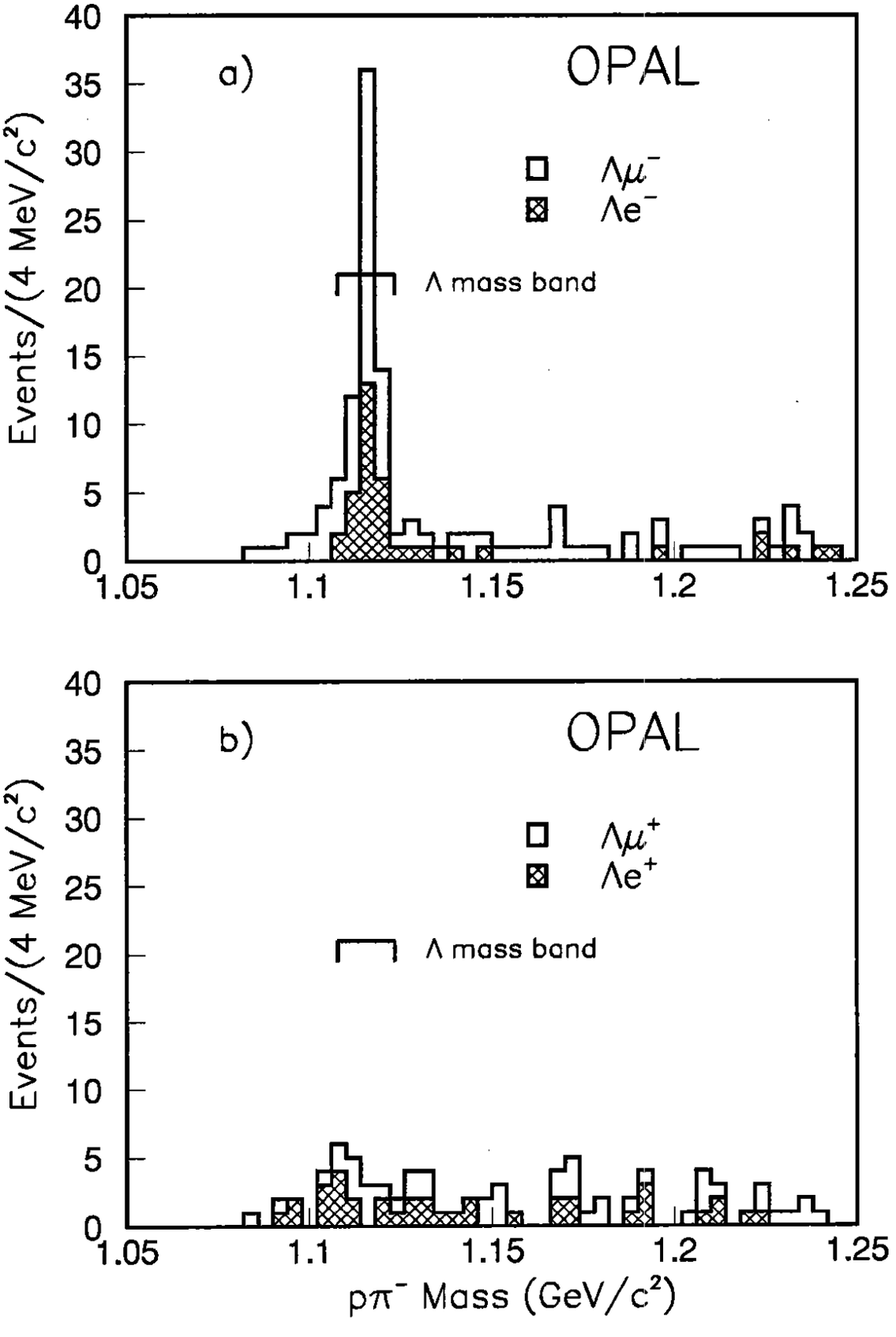
a)
OPAL
$\Lambda\mu^-$
Λe^-
Λ mass band
Events/(4 MeV/c²)
b)
OPAL
$\Lambda\mu^+$
Λe^+
Λ mass band
Events/(4 MeV/c²)
pπ⁻ Mass (GeV/c²)

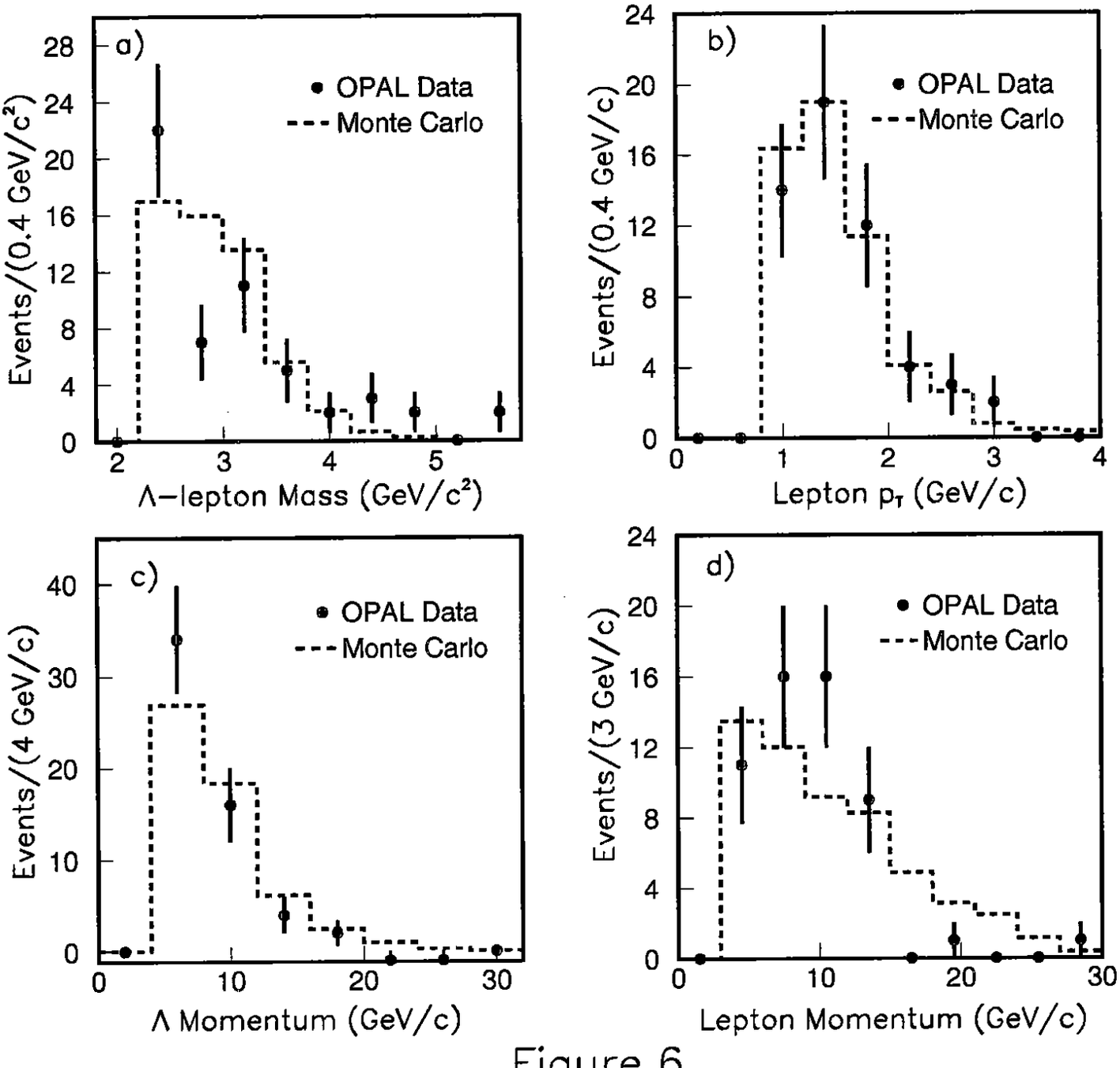
a)
OPAL Data
Monte Carlo
Events/(0.4 GeV/c²)
Λ–lepton Mass (GeV/c²)
b)
OPAL Data
Monte Carlo
Events/(0.4 GeV/c)
Lepton p_T (GeV/c)
c)
OPAL Data
Monte Carlo
Events/(4 GeV/c)
Λ Momentum (GeV/c)
d)
OPAL Data
Monte Carlo
Events/(3 GeV/c)
Lepton Momentum (GeV/c)

Figure 6